

Crystallization of Low-Density Polyethylene- and Linear Low-Density Polyethylene-Rich Blends

KATE M. DRUMMOND,¹ JEFFERSON L. HOPEWELL,² ROBERT A. SHANKS¹

¹ CRC for Polymers Pty. Ltd., Department of Applied Chemistry, RMIT University, GPO Box 2476V, Melbourne, Victoria, 3001, Australia

² CRC for Polymers Pty. Ltd., Polymer Technology Centre, RMIT University, Melbourne, Victoria, Australia

Received 21 October 1999; accepted 17 February 2000

ABSTRACT: The crystallization of a series of low-density polyethylene (LDPE)- and linear low-density polyethylene (LLDPE)-rich blends was examined using differential scanning calorimetry (DSC). DSC analysis after continuous slow cooling showed a broadening of the LLDPE melt peak and subsequent increase in the area of a second lower-temperature peak with increasing concentration of LDPE. Melt endotherms following stepwise crystallization (thermal fractionation) detailed the effect of the addition of LDPE to LLDPE, showing a nonlinear broadening in the melting distribution of lamellae, across the temperature range 80–140°C, with increasing concentration of LDPE. An increase in the population of crystallites melting in the region between 110 and 120°C, a region where as a pure component LDPE does not melt, was observed. A decrease in the crystallite population over the temperature range where LDPE exhibits its primary melting peaks (90–110°C) was noted, indicating that a proportion of the lamellae in this temperature range (attributed to either LDPE or LLDPE) were shifted to a higher melt temperature. © 2000 John Wiley & Sons, Inc. *J Appl Polym Sci* 78: 1009–1016, 2000

Key words: LLDPE; LDPE; polyethylene blends; thermal fractionation; DSC

INTRODUCTION

Linear low-density polyethylene (LLDPE), a copolymer of ethylene and an α -olefin, with short-chain branching is used extensively as packaging film due to its excellent mechanical properties, such as tear and impact strength, as well as high tensile strength at break.^{1,2} However, difficulties can arise during processing of LLDPE film due to a narrow molar mass distribution, causing an elevation in the melt viscosity and a lowering of the melt strength of the polymer.² Blending small amounts (typically up to 30% w/w) of low-density

polyethylene (LDPE), a polyethylene with both short- and long-chain branching, alleviates processing difficulties by increasing the extensional viscosity and, therefore, the bubble stability during blown film extrusion of the material.³ Furthermore, the addition of LDPE to LLDPE has been shown to improve the optical properties of the blown film while maintaining the superior mechanical properties exhibited by LLDPE.^{2,4,5}

The improvement in the optical properties of LLDPE with the addition of LDPE is thought to be due to a nucleating effect; both LDPE² and LLDPE⁵ have been proposed as acting as the nucleating agent. A number of studies have examined the morphology and crystallization behavior of LDPE–LLDPE blends.^{4–10} It has been shown that the degree of phase segregation and cocrys-

Correspondence to: K. M. Drummond (kate.drummond@rmit.edu.au).

Journal of Applied Polymer Science, Vol. 78, 1009–1016 (2000)
© 2000 John Wiley & Sons, Inc.

tallization of PE blends is dependent on the rate of crystallization, as shown by Morgan et al. for linear polyethylene (HDPE)–LDPE solution-mixed blends¹¹ and Müller and coworkers for LLDPE–LDPE-rich melt-mixed blends.⁵ The thermal history of the blend has also been shown to influence the microstructure as illustrated by Tsukame et al. for a range of PE blends.⁹ An intermediate (metastable) structure in the form of a shoulder was observed in the DSC thermogram for LDPE–LLDPE blends upon first heating, which they attributed to an entanglement of PE chains. This shoulder was replaced by a distinct second peak following additional heating.

In a study of LDPE–butene LLDPE blends using DSC and light-scattering techniques, it was proposed that, upon crystallization of LLDPE from the molten state, volume-filling spherulites are generated, with the LDPE then crystallizing within these spherulites.^{7,12} Two crystal populations were observed by Hill and Puig, following rapid quenching of solution-mixed LDPE–octene LLDPE blends for primarily LDPE-rich blends and it is argued that this indicates that the blends were phase-separated in the melt prior to quenching.⁶ It was also proposed that branch number, and not branch type, was the important factor in the occurrence of phase separation in the melt. The microstructure and mechanical properties of melt-extruded octene LLDPE–LDPE-rich blends were examined in a study by Müller and coworkers.⁵ The miscibility of the blends was shown to be strongly dependent on the composition and temperature. Upon rapid quenching of these blends, two distinct phases, one attributed to LLDPE and the other LDPE, were noted, while at slower cooling rates, an additional melt endotherm was observed, suggesting the development of a miscible phase. The tensile properties of these blends indicated that the blends were compatible.⁵ Electron microscopy results for isothermally crystallized LLDPE–LDPE blends have suggested that remixing occurs during crystallization.⁶

The miscibility of commercial LDPE–butene LLDPE blends was also examined using temperature-rising elution fractionation (TREF), a technique which fractionates polymers according to the crystallizability of the polymers.⁸ Solution-mixed TREF fractions of LDPE and LLDPE of similar branch number were observed to exhibit greater miscibility than those of mixed fractions of varying branch number, indicating cocrystallization between molecular segments with similar distances between branches.

Stepwise crystallization and successive self-annealing techniques using differential scanning calorimetry were performed on PEs to examine the heterogeneity of comonomer distribution and the effect of branching and catalysis on the crystallization.^{13–16} Recently, these techniques were also used to examine the crystallization of PE blends, such as very low density polyethylene (VLDPE)–LLDPE blends¹⁷ and LLDPE–HDPE blends.^{18,19} Both thermal fractionation and successive self-nucleation techniques fractionate according to the size of the linear segments in the polymer and provide information on the distribution of the lamella thickness.^{13,14} In thermal fractionation, the polymer is isothermally crystallized and annealed at a series of temperatures below the melting temperature of the polymer. In successive self-annealing, the polymer is also annealed at a temperature below the melting temperature of the polymer; however, on completion of each annealing step, the polymer is cooled to ambient temperature. The polymer is then heated (and annealed) at a lower temperature and the cycle repeated. The polymer is able to self-nucleate at each temperature. The subsequent melting of the polymer following either fractionation technique will detail the distribution of the crystallites as a function of size.²⁰

In this study, the crystallization behavior of LDPE–LLDPE-rich blends (up to 30% LDPE) made from commercial PEs was examined using DSC both after continuous slow cooling and stepwise isothermal crystallization (thermal fractionation) over a wide temperature range, including that above the crystallization temperature of LDPE. In particular, the change in the distribution of the lamellae with the addition of LDPE to LLDPE was examined.

EXPERIMENTAL

Materials

Commercial grades of a gas-phase polymerized hexene LLDPE and an LDPE obtained from Orica Pty. Ltd. (Melbourne, Australia) were used in this study. The properties of these polymers are detailed in Table I.

PE Blending

Granular LLDPE and LDPE of a predetermined mass were tumble-mixed prior to addition to the

Table I Properties of the LLDPE and LDPE Used in the Study

| Material | MFI (g 10 min ⁻¹) | ρ (kg m ⁻³) | T_m (°C) | M_n (g mol ⁻¹) | M_w (g mol ⁻¹) | M_w/M_n (g mol ⁻¹) | Total Branch Content (1000 C ⁻¹) |
|--------------|----------------------------------|---------------------------------|---------------|---------------------------------|---------------------------------|-------------------------------------|--|
| Hexene LLDPE | 0.8 | 920 | 123.7 | 46,800 | 146,000 | 3.1 | 19.9 |
| LDPE | 1.7 | 921 | 106.7 | 25,200 | 78,700 | 31.0 | 20.1 |

hopper of the extruder. The PE blends were processed using a Brabender twin-screw extruder. A screw speed of 100 rpm was used and the temperature profile was set to achieve a melt temperature of approximately 220°C in the mixing zones of the extruder. The extruded strand of polymer was cooled to ambient temperature and pelletized.

Thermal Fractionation Method

Weighed polymer samples (2–5 mg) were crimp-sealed in 30- μ L aluminum DSC pans. Polymer samples were thermally fractionated using a Perkin-Elmer Pyris 1 differential scanning calorimeter. The thermal fractionation procedure was performed using a nominal cooling rate of 200°C min⁻¹, an isothermal crystallization time of 50 min, and a 4°C crystallization step. Included in the thermal fractionation program was an initial step to remove the thermal history of the polymer. This was achieved by heating the polymer to 160°C for 5 min. The temperature was then decreased to the initial temperature (122°C) of the thermal fractionation procedure, at a nominal rate of 200°C min⁻¹ and annealed at this temperature for 50 min. Subsequent stepwise crystallization steps of 4°C with a nominal cooling rate of 200°C min⁻¹ were used, until a temperature of 50°C was reached. The sample was then cooled to ambient temperature.

Thermal Analysis

Melt endotherms of the LDPE-LLDPE blends were recorded using a Perkin-Elmer DSC-7 instrument over a temperature range of 40 and 160°C for a heating rate of 10°C min⁻¹. The temperature and enthalpy of the DSC instruments were calibrated using an indium standard. Thermal analyses were performed under a nitrogen purge. Both thermal fractionation and subsequent thermal analysis experiments were operated with a cold finger of ice/water (<5°C) in the DSC instruments.

RESULTS AND DISCUSSION

Typical melt endotherms of hexene LLDPE and LDPE, following crystallization from 160 to 40°C at a rate of 10°C min⁻¹, are shown in Figures 1 and 2 (dashed lines). Both PEs exhibit a single melt endotherm with a broad tail on the low-temperature side of the peak. The observed tailing to the peak indicates the presence of lamellae containing polymer segments of varying branching density in both PEs.²⁰ The cause of the dispersity in the branching density is related to the conditions and type of catalyst used in the polymerization process.^{14,21,22} In the polymerization of LLDPE, the availability of multiple active sites on the Ziegler-Natta catalyst results in the heterogeneous distribution of the comonomer, producing a broad range of crystallite sizes. LDPE is produced by a free-radical polymerization process, using a peroxide catalyst, under high temperature and pressure. These conditions favor the formation of both long- and short-chain branching.

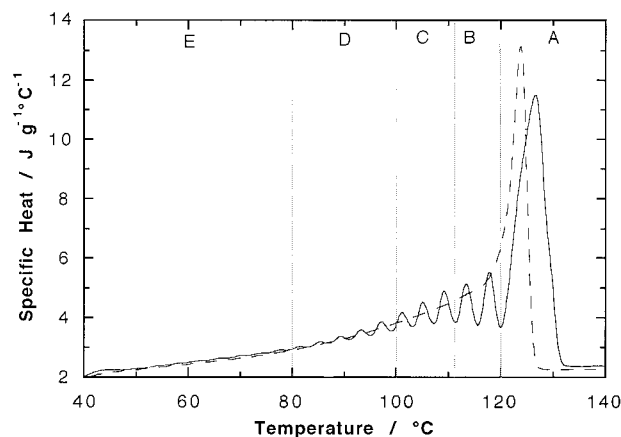


Figure 1 (—) A specific heat curve of hexene LLDPE following thermal fractionation. Also shown is (- - -) a specific heat curve following crystallization at 10°C min⁻¹. Both specific heat curves were recorded at a rate of 10°C min⁻¹.

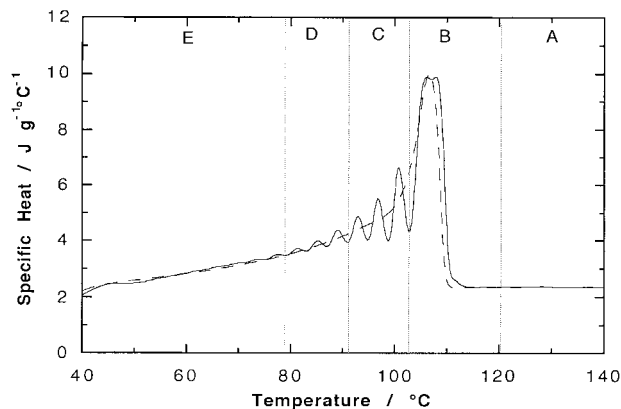


Figure 2 A specific heat curve of LDPE following thermal fractionation (—). Also shown is (---) a specific heat curve following crystallization at $10^{\circ}\text{C min}^{-1}$. Specific heat curves were recorded at a rate of $10^{\circ}\text{C min}^{-1}$.

The specific heat curves of LLDPE and LDPE following thermal fractionation treatment are also shown in Figures 1 and 2 (solid lines). The specific heat curves of both PEs following thermal fractionation display a series of well-resolved peaks, representing crystallite fractions of a specific branching density.²³ The isothermal crystallization time of 50 min is clearly sufficient time to allow the polymer segments to crystallize for a given crystallization temperature. This average cooling rate of $0.08^{\circ}\text{C min}^{-1}$ (i.e., 50 min per 4°C step) is of the order often used during TREF crystallization.²⁴ In this study, it was found that a rate of $0.08^{\circ}\text{C min}^{-1}$ produced adequate separation of the melting peaks, while slower rates did not provide any significant improvement in the resolution of the peaks.

Between a temperature range of 80 and 140°C , 11 peaks for the hexene LLDPE and seven peaks for the LDPE were produced. The number of peaks observed in the melt endotherms of the polymers following thermal fractionation correspond to the number of crystallization steps in the thermal fractionation program below the onset of the polymer's crystallization temperature. The specific heat curve of LDPE following thermal treatment displays a narrower crystallization temperature range than that of LLDPE, indicating a narrower size distribution of crystallites. This is to be expected due to the narrower distribution of short-chain branches formed in the free-radical polymerization process of LDPE compared with LLDPE produced using the Ziegler–Natta catalyst.

Analogous to the elution temperature in TREF analysis, the highest melting temperature peak of LLDPE following thermal fractionation is predominantly composed of lamellae from substantially linear macromolecules.^{14,23,25} The subsequent peaks of the LLDPE melt scan toward lower melting temperatures are composed of lamellae containing polymer chains with a higher degree of branching. Similarly, the branch content of LDPE will increase with decreasing melt temperature.

It has been shown that the degree of branching obtained for fractionated LLDPEs using TREF can be correlated with the melt temperature obtained from DSC.^{14,22,26} The relationship between the melt temperature and the degree of branching was shown to be linear for fractionated LLDPEs^{8,26–28} and is dependent on the comonomer of the LLDPE.^{26–28} TREF analysis revealed that for a specific degree of short-chain branching (SCB) between 1 and 30 per 1000 carbons the melting temperature of fractionated LLDPEs increases according to the comonomer butene followed by hexene and octene.²⁶ Using TREF data for hexene LLDPE from the literature,²⁶ the degree of SCB per 1000 carbons for a temperature range of 90 – 140°C can be approximated for a given melting temperature (T_m):

$$T_m = -1.7\text{SCB} + 134^{\circ}\text{C} \quad (1)$$

Using this equation, the degree of branching for the highest melting temperature peak of hexene LLDPE (126°C) is estimated to be five branches per 1000 carbons, while the lowest-temperature peak (82°C) is estimated to be 30.

Specific heat curves of a series of LDPE–LLDPE blends for an LDPE concentration range between 2 and 30% following crystallization at $10^{\circ}\text{C min}^{-1}$ are shown in Figure 3 (dashed lines). The standard melt endotherms (without thermal treatment) show that at LDPE concentrations below 10% there is a broadening of the LLDPE melting peak, while at concentrations above 10%, a second melting peak develops at $\sim 105^{\circ}\text{C}$, although not well resolved from the LLDPE melting peak. The standard DSC curves indicate that the melting temperature of the LLDPE peak does not change significantly over the LDPE concentration range studied.

The specific heat curves of the LDPE–LLDPE-rich blends following thermal fractionation are shown in Figure 3 (solid lines). They illustrate a

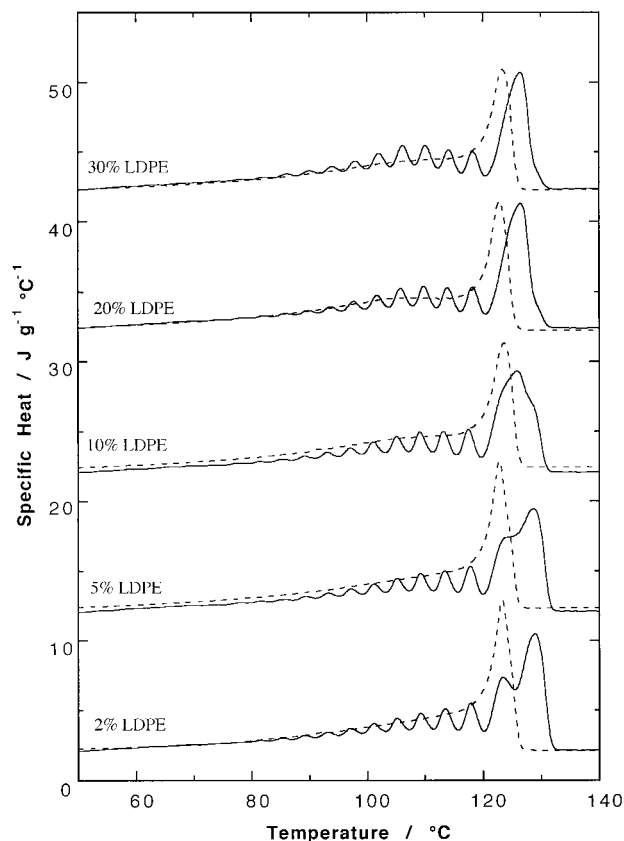


Figure 3 Specific heat curves collected at a rate of $10^{\circ}\text{C min}^{-1}$ for a range of LDPE–LLDPE blends after (—) thermal fractionation and (---) crystallization at $10^{\circ}\text{C min}^{-1}$. The curves are separated by 10 additive units.

series of well-resolved peaks, indicating that material of similar branch content from both LDPE and LLDPE is able to crystallize without hindrance in these blends. The series of curves show a reduction in the size of the primary LLDPE crystallization peak, with increasing concentration of LDPE. The population of the crystallites is clearly shifted to a lower temperature range, due to the lower crystallization temperature of LDPE. Comparison of the specific heat curves obtained following crystallization at a cooling rate of $10^{\circ}\text{C min}^{-1}$ with specific heat curves obtained following thermal fractionation shows that the method of stepwise crystallization enables segmental segregation of the blend into components of similar branch numbers to occur.

The intermittent occurrence ($\sim 50\%$ of the scans) of a shoulder on the primary LLDPE melting peak was observed in the specific heat curves of the fractionated blends for LDPE concentrations 10% and below. Figure 4 illustrates the vari-

ation in the shape of the primary crystallization peak of a 5% LDPE–LLDPE blend for two samples. The origin of this shoulder is not fully understood. Splitting of the primary melt endotherm was not observed for LDPE concentrations above 10%. Also, splitting of the melt endotherm was not apparent following crystallization at $10^{\circ}\text{C min}^{-1}$; therefore, it would appear not to be attributed to recrystallization, as the splitting would be expected to become more pronounced with an increase in the crystallization rate. In a study of LDPE-rich blends with octene LLDPE using standard DSC techniques,⁵ additional peaks in the melt endotherms were observed following cooling at $10^{\circ}\text{C min}^{-1}$. It was proposed that during slow crystallization the melt remixes to form a third (miscible) phase.

The influence of LDPE on the crystallization of LLDPE in the blend was examined by comparison of the specific heat curves of the thermally fractionated blends with the calculated specific heat curves, as generated based on the additivity rule. Shown in Figure 5 are the calculated specific heat curves (dashed lines) along with the experimental specific heat curves (solid lines) for the blends following thermal treatment. The figure illustrates that for all blends studied there is a considerable difference between the experimental and calculated specific heat curves, even at concentrations as low as 2% LDPE. The irregular appearance of the shoulder is not predicted by additivity, and as a consequence, the specific heat of these experimental curves is lower for LDPE concentrations 10% and below. For concentra-

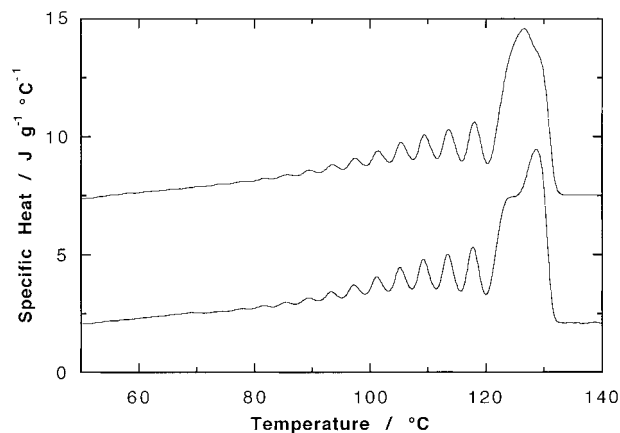


Figure 4 Specific heat curves of a 5% LDPE–LLDPE blend following thermal treatment, showing the variation in shape of the primary crystallization peak of LLDPE.

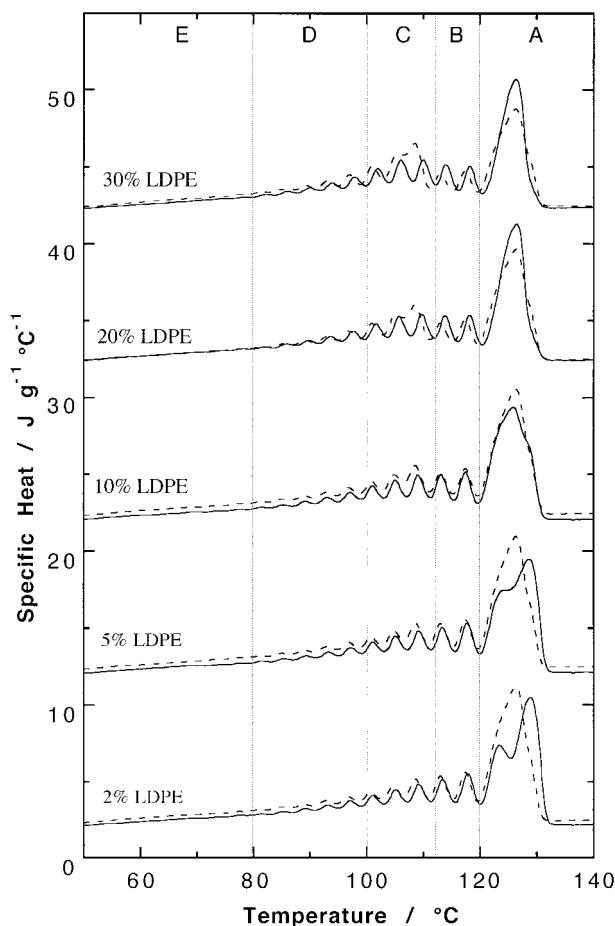


Figure 5 Comparison of the (—) observed specific heat curves with (---) calculated specific heat curves for a series of LDPE-LLDPE blends following thermal fractionation. The curves are separated by 10 additive units.

tions above 10% LDPE, the observed specific heat curve was typically higher than that of the additive curve. Interestingly, greater resolution of the melting peaks over the temperature range of the primary LDPE melt peaks (90–105°C) than that predicted from the additive curve for concentrations above 10% LDPE was attained experimentally. It has also been shown that thermal fractionation of branched VLDPE-LLDPE blends produces greater resolution experimentally than that estimated from additivity for concentrations of 20% and above of VLDPE.¹⁷

Partial area analysis of the thermally fractionated polymers for the experimental specific heat curves of the blends and the pure components, for a given temperature range, are shown in Table II. The population of crystals of a particular melting distribution is proportional to the partial area for

a given temperature range. The temperature regions designated A–E are marked on Figures 1, 2, and 5. Based on the observations of the specific heat curves of the pure polymers following thermal fractionation (Figs. 1 and 2), material melting in regions A and B will be presumably crystals attributed to LLDPE, as these regions are above the melting temperature of LDPE. LDPE will predominantly melt between the temperatures of 78 and 110°C (regions C and D), with the highest-temperature LDPE crystallites melting between 98 and 110°C (region C). For material melting at temperatures below 80°C (region E), PE crystallites will be composed of highly branched macromolecules. Partial area analysis of region E revealed that for LLDPE, LDPE, and their blends the total partial area comprised less than 11%. Also, it was found that the shoulder/splitting of the primary LLDPE melting peak did not significantly affect the calculated partial area, as shown in Table II for the 5% LDPE-LLDPE blend.

Based on the assumption that the specific heat curves of the LDPE-LLDPE-rich blends after thermal treatment follows additivity, the ratio of the partial areas between the experimental and calculated data should yield a value of 1. A ratio greater (less) than 1 indicates an increase (decrease) in the population of the crystals. The ratio of the partial areas of the experimental data to that of the additive data is shown as a function of region in Table III. The discrepancy between the experimental and calculated partial areas, for the entire concentration range studied, is clearly illustrated. The experimental results show an increase in the population of crystals (ratio >1), in regions A and B, from as low as 2% LDPE. In addition, the concentration of crystals (ratio <1) in region C is lower, a region where LDPE displays its primary melting peak. The results show that the addition of LDPE produces a general shift in the population of the crystallites to a higher melting temperature range.

LDPE does not melt in the temperature range of regions A and B as a pure polymer (Fig. 2), which would indicate that either the presence of LDPE is affecting the crystallization of LLDPE segments to a higher temperature or the presence of LLDPE is nucleating the crystallization of LDPE to a higher temperature. Region D does not deviate significantly from a ratio of 1, confirming that it is the more linear domains that are affected. It should be noted that region E, which is typically composed of less than 11% of the total

Table II Partial Areas of LLDPE, LDPE, and Their Blends for Selected Temperature Ranges, Designated A–E as Calculated from the Specific Heat Curves Following Thermal Fractionation

| Blend | Partial Area (%) | | | | |
|----------|------------------|------|------|------|------|
| | A | B | C | D | E |
| LLDPE | 44.6 | 14.5 | 17.1 | 15.5 | 8.3 |
| LDPE | 0.0 | 0.0 | 51.7 | 32.4 | 15.9 |
| 2% LDPE | 44.0 | 15.3 | 17.2 | 15.4 | 8.1 |
| 5% LDPE | 43.8 | 14.4 | 17.1 | 16.3 | 8.4 |
| | 43.4 | 14.5 | 18.0 | 16.1 | 8.0 |
| 10% LDPE | 41.5 | 13.7 | 19.1 | 17.5 | 8.2 |
| 20% LDPE | 37.9 | 13.5 | 20.6 | 18.9 | 9.1 |
| 30% LDPE | 33.6 | 12.5 | 22.9 | 20.3 | 10.8 |

partial area, will have a greater error as the peaks are not as well resolved in this region, so it can be assumed that these molecules are also not significantly affected.

The presence of LDPE may assist the physical separation of the linear and highly branched domains of LLDPE, allowing the crystallization of the linear LLDPE segments at a higher temperature than that which is observed in LLDPE alone, causing an increase in the melting temperature. On the other hand, it may be that a number of longer linear segments in LDPE that are too few to crystallize by themselves are able to cocrystallize in the presence of LLDPE. Either scenario would result in a shift in the lamellae distribution and, therefore, the partial area to a higher melting temperature.

In a study of melt-extruded HDPE–LDPE blends, it was proposed that when the temperature is held above the highest crystallization temperature of branched PE the existing lamellae act as nuclei for the crystallization of branched PE lamellae.²⁹ Similar findings were also reported by

Puig for solution-mixed branched PE and HDPE blends following isothermal crystallization.³⁰ In studies of the crystallization of LLDPE-rich–HDPE blends using a successive self-nucleation technique^{18,19} and VLDPE-rich–LLDPE blends using thermal fractionation,¹⁷ cocrystallization was also observed to occur. In particular, it was noted that in the study of the LLDPE-rich–HDPE blends that the partial area of the primary melt temperature of LLDPE was greater than that calculated from the additivity rule. It was proposed that cocrystallization was occurring between LLDPE and HDPE crystals at this temperature range (11°C) for the LLDPE-rich–HDPE blends. Similarly, in HDPE-rich–LLDPE blends, a greater partial area was observed for those crystals fused at the primary HDPE crystallization peak (124°C), although to a lesser extent.

CONCLUSIONS

Analysis of the melt endotherms of LDPE–LLDPE blends following stepwise crystallization

Table III Ratio Between the Experimental and Calculated Partial Areas as a Function of Region for LDPE–LLDPE-rich Blends

| Blend | Partial Area _{exp} /Partial Area _{calcd} | | | | |
|----------|--|------|------|------|------|
| | A | B | C | D | E |
| 2% LDPE | 1.01 | 1.08 | 0.97 | 0.97 | 0.95 |
| 5% LDPE | 1.03 | 1.05 | 0.91 | 1.00 | 0.97 |
| | 1.02 | 1.05 | 0.95 | 0.99 | 0.92 |
| 10% LDPE | 1.03 | 1.05 | 0.93 | 1.02 | 0.90 |
| 20% LDPE | 1.06 | 1.16 | 0.86 | 1.00 | 0.93 |
| 30% LDPE | 1.08 | 1.23 | 0.83 | 0.99 | 1.00 |

(thermal fractionation) has provided a more detailed understanding of the branching distribution than has standard thermal analysis alone. Following thermal fractionation, the addition of LDPE to LLDPE to form an LDPE–LLDPE-rich blend was shown to alter the crystallization, shifting the population of crystals to an elevated melting temperature, from concentrations as low as 2% LDPE. It is proposed that LDPE is able to separate the more highly branched LLDPE molecules, thereby allowing the molecules with longer linear segments to crystallize to a greater extent. An alternative explanation is that there are molecules with long segments between branches in LDPE that can cocrystallize with the longer unbranched segments of LLDPE but are too few to crystallize within pure LDPE.

REFERENCES

1. Utracki, L. A. *Polymer Alloys and Blends: Thermodynamics and Rheology*; Hanser: Munich, 1989.
2. ICI Alkatuff™ and Alkathene™ Polyethylene, Booklet No. 3; ICI Australia Pty. Ltd., 1992.
3. Speed, C. S. *Plast Eng* 1982, 39.
4. Schlund, B.; Utracki, L. A. *J Polym Eng Sci* 1987, 27, 359.
5. Müller, A. J.; Balsamo, V.; Rosales, C. M. *Polym Networks Blends* 1992, 2, 215.
6. Hill, M. J.; Puig, C. C. *J Appl Polym Sci* 1997, 65, 1921.
7. Kyu, T.; Hu, S.-R.; Stein, R. S. *J Polym Sci Part B Polym Phys* 1987, 25, 89.
8. Joskowicz, P. L.; Muñoz, A.; Barrera, J.; Müller, A. *J Macromol Chem Phys* 1995, 196, 385.
9. Tsukame, T.; Ehara, Y.; Shimizu, Y.; Kutsuzawa, M.; Saitoh, H.; Shibasaki, Y. *Thermochim Acta* 1997, 299, 27.
10. Prasad, A. *J Polym Eng Sci* 1998, 38, 1716.
11. Morgan, R. L.; Hill, M. J.; Barham, P. J. *Polymer* 1999, 40, 337.
12. Ree, M.; Kyu, T.; Stein, R. S. *J Polym Sci Part B Polym Phys* 1987, 25, 105.
13. Varga, J.; Menczel, J.; Solth, A. *J Therm Anal* 1979, 17, 333.
14. Balbontin, G.; Camurati, I.; Dall'Occo, T.; Zeigler, R. C. *J Mol Catal A Chem* 1995, 98, 123.
15. Balbontin, G.; Camurati, I.; Dall'Occo, T.; Finotti, A.; Franzese, R.; Vecellio, G. *Makromol Chem* 1994, 219, 139.
16. Keating, M. Y.; McCord, E. F. *Thermochim Acta* 1994, 243, 129.
17. Shanks, R. A. Amarsinghe, G. *Polymer*, in press.
18. Müller, A. J.; Arnal, M. L.; Méndez, G.; Sánchez, J. J. In *37th International Symposium on Macromolecules*, 1988; p 85.
19. Arnal, M. L.; Sánchez, J. J.; Müller, A. J. *Soc Plast Eng* 1999, 2329.
20. Wunderlich, B. In *Macromolecular Physics*; Academic: New York, 1980; Vol. 3; p 134.
21. Kakugo, M.; Naito, Y.; Mizunuma, K.; Miyatake, T. *Macromolecules* 1982, 15, 1150.
22. Usami, T.; Gotoh, Y.; Takayama, S. *Macromolecules* 1986, 19, 2722.
23. Adisson, E.; Ribeiro, M.; Deffieux, A.; Fontanille, M. *Polymer* 1992, 33, 4337.
24. Monrabel, B. *J Appl Polym Sci* 1994, 52, 491.
25. Schouterden, P.; Groeninckx, G.; Van der Heijden, B.; Jansen, F. *Polymer* 1987, 28, 2099.
26. Hosoda, S. *Polym J* 1988, 20, 383.
27. Mandelkern, L. In *Comprehensive Polymer Science, The Synthesis, Characterization, Reactions and Applications of Polymers*; Allen, G.; Bevington, J. C., Eds.; Pergamon: Oxford, UK, 1989.
28. Alamo, R.; Domsy, R.; Mandelkern, L. *J Phys Chem* 1984, 88, 6587.
29. Minick, J.; Moet, A.; Baer, E. *Polymer* 1995, 36, 1923.
30. Puig, C. C. *Polym Bull* 1996, 36, 361.